In situ high-temperature X-ray diffraction characterization of silver sulfide, Ag$_2$S

Thomas Blanton[a)]
Eastman Kodak Company, Rochester, New York 14650-2106

Scott Misture
Alfred University, Alfred, New York 14802

Narasimharao Dontula
Eastman Kodak Company, Rochester, New York 14650-2106

Swavek Zdzieszynski
Alfred University, Alfred, New York 14802

Silver sulfide, Ag$_2$S, is most commonly known as the tarnish that forms on silver surfaces due to the exposure of silver to hydrogen sulfide. The mineral acanthite is a monoclinic crystalline form of Ag$_2$S that is stable to 176 °C. Upon heating above 176 °C, there is a phase conversion to a body-centered cubic (bcc) form referred to as argentite. Further heating above 586 °C results in conversion of the bcc phase to a face-centered cubic (fcc) phase polymorph. Both high-temperature cubic phases are solid-state silver ion conductors. *In situ* high-temperature X-ray diffraction was used to better understand the polymorphs of Ag$_2$S on heating. The existing powder diffraction file (PDF) entries for the high-temperature fcc polymorph are of questionable reliability, prompting a full Rietveld structure refinement of the bcc and fcc polymorphs. Rietveld analysis was useful to show that the silver atoms are largely disordered and can only be described by unreasonably large isotropic displacement parameters or split site models. © *2011 International Centre for Diffraction Data.* [DOI: 10.1154/1.3583564]

I. INTRODUCTION

Solid ionic conductors, also called solid electrolytes, transport electric current by means of ions. Ionic conduction in solid electrolytes typically peaks if a partial lattice of a solid compound undergoes a transition, usually at elevated temperature, to a quasimolten state (Rickert, 1978). A large number of silver ion conductors have been studied based on silver iodide, AgI (Takahashi, 1973). At room temperature AgI can be found in both a hexagonal (β-AgI) and a face-centered cubic (γ-AgI) polymorphic form. Upon heating to 147 °C, AgI transforms to a body-centered cubic (α-AgI) polymorph that is an ionic conductor (Takahashi, 1978). Although the structure of α-AgI is presented as having two AgI entities in a bcc unit cell, the Ag ions have been found to be distributed statistically over 42 available sites (Strock, 1936; Hoshino, 1957). Neutron diffraction studies of α-AgI indicate that silver ions are preferentially found in ellipsoidal regions of space centered at tetrahedral sites, and there is a significant anharmonic contribution to the thermal vibrations in the direction of the octahedral sites. This model suggests silver ions move along the ⟨100⟩ direction in channel-like diffusion paths (Eckold *et al.*, 1976).

Silver chalcogenides (silver sulfide Ag$_2$S, silver selenide Ag$_2$Se, and silver telluride, Ag$_2$Te) are also known to be solid-state ionic conductors with mobile silver ions along with electrons and/or holes (Okazaki, 1967). In the case of Ag$_2$S, the ionic conductivity, σ_i, particularly at elevated temperature, can be large (>5 Ω^{-1} cm^{-1}), putting this material into the category of superionic conductors (Miyatani, 1981). At room temperature, Ag$_2$S has a monoclinic structure (space group $P2_1/n$, $Z=4$) and is referred to as β-Ag$_2$S, also known by its mineral name acanthite. Above 176 °C, Ag$_2$S undergoes a structural phase transition (Djurle, 1958), becoming body-centered cubic (space group $Im\bar{3}m$, $Z=2$), referred to as α-Ag$_2$S, with the mineral name argentite. Upon further heating, >586 °C, a second phase transition occurs for Ag$_2$S (Frueh, 1961). This third polymorph has a face-centered cubic structure (space group $Fm\bar{3}m$, $Z=4$). There is no mineral name for this FCC Ag$_2$S polymorph, and it is suggested here to refer to this phase as γ-Ag$_2$S. It is the bcc and fcc polymorphs of Ag$_2$S that are of interest as ionic conductors.

The original research project that initiated this study was to investigate possible methods of incorporating an ionic conducting species of Ag$_2$S in a host polymer to generate a conductive extruded film. Evaluation of reference data in the powder diffraction file (PDF) (ICDD, 2010), revealed many calculated diffraction patterns for the high-temperature Ag$_2$S phases. However, high-quality experimental patterns and subsequent refined crystal structure data were not available for the bcc and fcc polymorphs. In an effort to enhance the reference data in the PDF, *in situ* high-temperature XRD data were collected for Ag$_2$S, with Rietveld refinement results for the β-Ag$_2$S, α-Ag$_2$S, and γ-Ag$_2$S phases reported as part of this study.

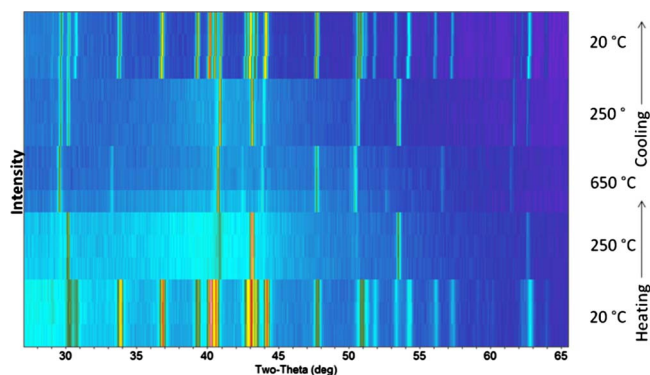[a)]Author to whom correspondence should be addressed. Electronic mail: thomas.blanton@kodak.com

Figure 1. (Color online) Film strip plot of *in situ* high-temperature XRD data for Ag_2S.

II. EXPERIMENTAL

A. Sample preparation

Into a glass vessel containing 100 ml de-ionized water was charged 12.845 g $AgNO_3$ (Eastman Kodak Co.). Into a second glass vessel containing 100 ml de-ionized water was charged 9.067g $Na_2S \cdot 9H_2O$ (Eastman Kodak Co.). Into a glass vessel containing 50 ml de-ionized water, the $AgNO_3$ and $Na_2S \cdot 9H_2O$ solutions were added simultaneously, resulting in the immediate formation of a black precipitate, Ag_2S. After stirring for 10 min, this dispersion was poured onto a vacuum filtration apparatus, and the precipitate was washed with 1000 ml de-ionized water. The precipitate was collected and placed in a ceramic bowl, followed by drying at 50 °C in a vacuum oven for 3 h. The dried powder was analyzed by XRD and identified as β-Ag_2S, acanthite PDF 00-014-0072 (ICDD, 2010).

B. X-ray diffraction

A Rigaku D2000 Bragg–Brentano diffractometer equipped with a copper rotating anode, diffracted beam graphite monochromator tuned to Cu $K\alpha$ radiation, and scintillation detector was used to confirm the phase identification of the black precipitate powder. *In situ* high-temperature XRD (HTXRD) experiments were performed using a Siemens D5000 diffractometer equipped with a custom XRD furnace (Misture, 2003), with measurements performed under pure N_2. Rietveld refinements were performed using the software program TOPAS (Bruker-AXS, 2009).
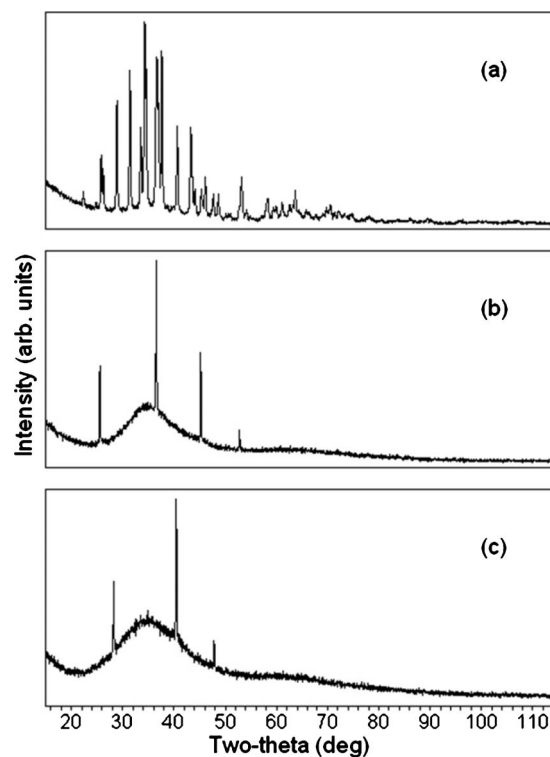

Figure 2. XRD patterns for Ag_2S collected at (a) 20 °C β phase, (b) 250 °C α phase, and (c) 650 °C γ phase.

III. RESULTS

An aliquot of β-Ag_2S powder was thermally processed using *in situ* high-temperature XRD. In Figure 1, HTXRD results plotted in film strip format show changes in the respective XRD patterns as Ag_2S is heated and then cooled. Corresponding one-dimensional diffraction patterns for data collected at 20, 250, and 650 °C (collected during heating) are presented in Figure 2. The nonambient XRD patterns have few diffraction peaks that help to explain the limited availability of good experimental reference patterns. At 250 °C, the observed diffraction peaks indicate that α-Ag_2S is present, consistent with the $\beta > \alpha$ transition at 176 °C. The diffraction peaks at 650 °C are due to γ-Ag_2S, as expected since the data were collected above the 586 °C $\beta > \gamma$ transition. The Ag_2S monoclinic > bcc > fcc phase transition order with increasing temperature is in contrast to other ionic conductors. For example, Ag_2Te transforms from monoclinic > fcc > bcc and AgI, CuBr, CuI, and CuCl all

TABLE I. Rietveld refinement structure of β-Ag_2S at 20 °C.

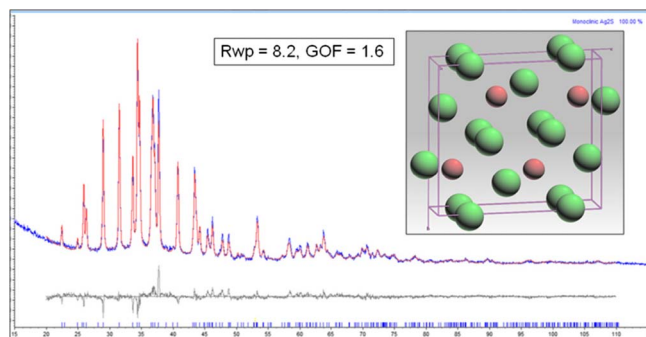| Crystal system		Monoclinic		a (Å)		4.2275(4)
Space group		$P2_1/n$		b (Å)		6.9303(5)
Z		4		c (Å)		8.2855(7)
Rwp		8.2		β (deg)		110.564(3)
GOF		1.6				
Site	Np	x	y	z	Occ.	Beq
Ag1	4	0.0412(7)	0.0154(5)	0.3075(4)	1	3.1(1)
Ag2	4	0.6456(8)	0.3222(4)	0.4369(4)	1	3.1(1)
S	4	0.272(2)	0.229(1)	0.128(1)	1	1

Figure 3. (Color online) Rietveld refinement (blue dots) vs raw data (red line) diffraction patterns for β-Ag_2S at 20 °C. Inset shows the refined β-Ag_2S crystal structure.
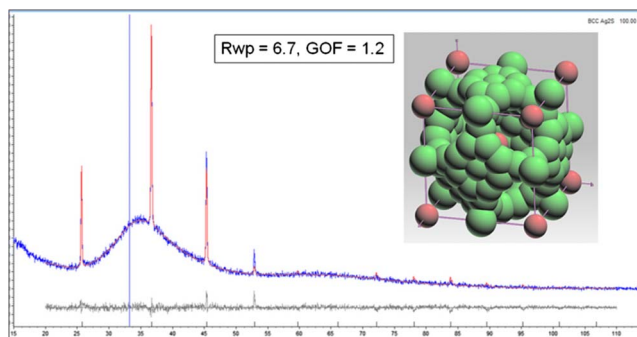

Figure 4. (Color online) Rietveld refinement (blue dots) vs. raw data (red line) diffraction patterns for α-Ag_2S at 250 °C. Inset shows the refined α-Ag_2S crystal structure.

show a high-temperature phase transition from fcc or hexagonal close packed (hcp) to bcc (Hull *et al.*, 2002).

Examination of the 250 °C [Figure 2(b)] and 650 °C [Figure 2(c)] XRD data show the presence of broad diffuse peaks at ~35 and 65° 2θ in both diffraction patterns. This observation was reported by Tsuchiya *et al.* (1978) in an early attempt to determine the crystal structure of α-Ag_2S. The diffuse scattering seen in α and γ-Ag_2S is attributed to Ag^+ ions in a highly disordered state resembling a liquidlike distribution. Powder neutron diffraction and molecular dynamics simulations (Hull *et al.*, 2002) found that Ag^+ ions predominantly reside in tetrahedral cavities of a S^{2-} lattice in α-Ag_2S and in both tetrahedral cavities and octahedral holes of a S^{2-} lattice in γ-Ag_2S. Using the partial structural results known for Ag_2S and the data collected in this study, structure refinement of the three Ag_2S phases was performed. Refinement was based on the sharp diffraction peaks, whereas the broad diffuse scattering was not modeled.

Refinement of the monoclinic β-Ag_2S phase yielded a structure solution similar to the structure reported by Sadanaga and Sueno (1967), although the refined structure from this study shows some differences in the *xyz* coordinates and required a large microstrain term. Refinement parameters are shown in Table I, and the Rietveld refinement diffraction pattern and β-Ag_2S structure are shown in Figure 3.

For α-Ag_2S at 250 °C, it was found that refining a previously reported structure model (Cava *et al.*, 1980) yielded unrealistic displacement parameters for the Ag ions of 17 and 6 $Å^2$ for the Ag atoms on the 12*d* and 6*b* Wyckoff sites. An improved refinement was obtained by allowing additional disorder in the system in the form of shifting the 12*d* Ag atoms to the 48*j* Wyckoff site and refining the occupancy. The result was a stable refinement with Rwp=6.7, GOF =1.2, and a refined stoichiometry of $Ag_{2.01}S$ without using constraints. The final structure parameters are shown in

TABLE II. Rietveld refinement structure of α-Ag_2S at 250 °C.

Crystal system	Cubic	a (Å)			4.8914(4)	
Space group	$Im\bar{3}m$					
Z	2					
Rwp	6.7					
GOF	1.2					
Site	Np	x	y	z	Occ.	Beq
Ag1	6	0	1/2	1/2	0.097(40)	1
Ag2	48	0	0.319(1)	0.430(1)	0.0715(9)	1
S	2	0	0	0	1	1

TABLE III. Rietveld refinement structure of γ-Ag_2S at 650 °C.

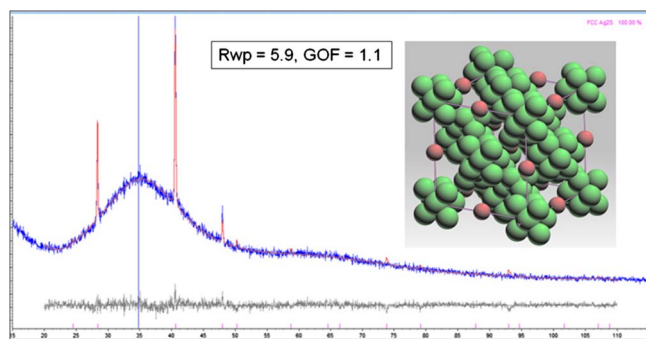| Crystal system	Cubic	a (Å)			6.2831(8)	
Space group	$Fm\bar{3}m$					
Z	4					
Rwp	5.9					
GOF	1.1					
Site	Np	x	y	z	Occ.	Beq
Ag1	8	1/4	1/4	1/4	0.088(70)	1
Ag2	32	0.303(4)	0.303(4)	0.303(4)	0.15(1)	1
Ag3	48	1/2	0.381(4)	0.381(4)	0.027(3)	1
S	4	0	0	0	1	1

Figure 5. (Color online) Rietveld refinement (blue dots) vs. raw data (red line) diffraction patterns for γ-Ag$_2$S at 650 °C. Inset shows the refined γ-Ag$_2$S crystal structure.

Table II and the Rietveld refinement diffraction pattern and α-Ag$_2$S structure are shown in Figure 4.

At 650 °C, the fcc γ-Ag$_2$S was also refined, beginning with the model of Frueh (1961). The result of the refinement was Rwp=6.1, GOF=1.1, but required unreasonable Beq values as high as 20 Å^2. Similar to α-Ag$_2$S, the Ag site was split to allow disorder along a logically possible Ag diffusion path, by adding a new Ag atom at the 48f site. The refinement proceeded without constraints to a final result shown in Table III, with Rwp=5.9 and GOF=1.1. The Rietveld refinement diffraction pattern and γ-Ag$_2$S structure are shown in Figure 5. A comparison of the newly adopted crystal structure to that reported by Frueh is shown in Figure 6. The model remains imperfect, as the refined model suggests some Ag deficiency, refining to Ag$_{1.7}$S. However, we interpret the refinement result as a substantial improvement over earlier models.

A possible explanation for the Ag deficiency in the refined γ-Ag$_2$S structure is the observation of Ag whiskers (confirmed by XRD) growing out of the surface of the Ag$_2$S powder at 650 °C (Figure 7). Silver whiskers are also known to form when silver electrical contacts are exposed to hydrogen sulfide (pollutant in air), resulting in short circuits in electrical components (Wikipedia, 2010).

IV. SUMMARY

Structures for acanthite (β), argentite (α), and fcc (γ) Ag$_2$S phases have been successfully refined using the HTXRD data. The resulting powder diffraction patterns are
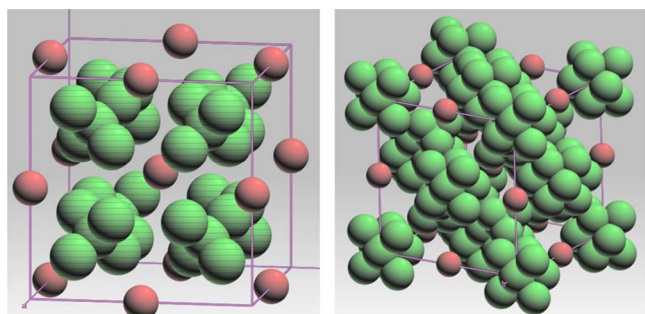

Figure 6. (Color online) Comparison of γ-Ag$_2$S crystal structure reported by Frueh (left) and the refined γ-Ag$_2$S crystal structure from this study with an additional Ag position (right).
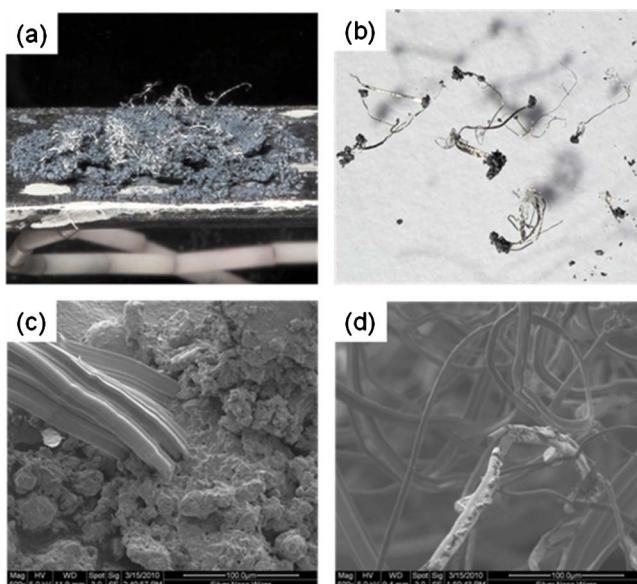

Figure 7. (Color online) Silver whiskers formed during HTXRD thermal processing of Ag$_2$S at 650 °C. (a) Ag$_2$S powder on a HTXRD heating strip, postheating; (b) silver whiskers attached to Ag$_2$S removed from the heating strip; (c) SEM micrograph (500×) of a silver whisker growing out of Ag$_2$S powder; (d) SEM micrograph (500×) of a bundle of silver whiskers.

an improvement to current patterns in the powder diffraction file and will be submitted for inclusion in the ICDD PDF database. The α and γ phases diffract very weakly and show diffuse scattering peaks due to mobile Ag atoms. These high-temperature phases are appropriate candidates for further study using maximum entropy modeling to determine the diffusion path(s) of Ag in the α and γ polymorphs. Heating up to 650 °C resulted in the formation of Ag whiskers, consistent with a refined silver-deficient structure for γ-Ag$_2$S.

Bruker-AXS (2009). TOPAS v. 4.0, Bruker-AXS, Madison, WI.

Cava, R. J., Reidinger, F., and Wuensch, B. J. (1980). "Single-crystal neutron diffraction study of the fast-ion conducting β-silver sulfide between 186 and 325 °C," J. Solid State Chem. 31, 69–80.

Djurle, S. (1958). "An x-ray study on the system Ag–Cu–S," Acta Chem. Scand. 12, 1427–1436.

Eckold, G., Funke, K., Klaus, J., and Lechner, R. E. (1976). "The diffusive motion of silver ions in α-silver iodide. Results from quasielastic neutron scattering," J. Phys. Chem. Solids 37, 1097–1103.

Frueh, A. J. (1961). "The use of zone theory in problems of sulfide mineralogy, Part III: Polymorphism of Ag$_2$Te and Ag$_2$S," Am. Mineral. 46, 654–660.

Hoshino, S. (1957). "Crystal structure and phase transition of some metallic halides. IV," J. Phys. Soc. Jpn. 12, 315–326.

Hull, S., Keen, D. A., Sivia, D. S., Madden, P., and Wilson, M. (2002). "The high-temperature superionic behaviour of Ag$_2$S," J. Phys.: Condens. Matter 14, L9–L17.

ICDD (2010). "Powder Diffraction File," edited by Dr. Soorya Kabekkodu, International Centre for Diffraction Data, Newtown Square, Pennsylvania.

Misture, S. T. (2003). "Large-volume atmosphere-controlled diffraction furnace," Meas. Sci. Technol. 14, 1091–1098.

Miyatani, S. (1981). "Ionic conductivity in silver chalcogenides," J. Phys. Soc. Jpn. 50, 3415–3418.

Okazaki, H. (1967). "Deviation from the Einstein relation in average crystals self-diffusion of Ag+ions in α-Ag$_2$S and α-Ag$_2$Se," J. Phys. Soc. Jpn. 23, 355–360.

Rickert, H. (1978). "Solid ionic conductors: Principles and applications," Angew. Chem., Int. Ed. Engl. 17, 37–46.

Sadanaga, S., and Sueno, S. (1967). "X-ray study on the α−β transition of Ag$_2$S," Mineral. J. 5, 124–143.

Strock, L. W. (**1936**). "Crystal structure of high-temperature silver iodide, α-AgI," Z. Phys. Chem. **B25**, 441–459.

Takahashi, T. (**1973**). "Solid silver ion conductors," J. Appl. Electrochem. **3**, 79–90.

Takahashi, T. (**1978**). "Silver and copper ion conductors in the solid state," Pure Appl. Chem. **50**, 1091–1098.

Tsuchiya, Y., Tamaki, S., Waseda, Y., and Toguri, J. M. (**1978**). "The structure of α-Ag$_2$S," J. Phys. C **11**, 651–659.

Wikipedia (**2010**). "Silver sulfide," http://en/wikipedia.org/wiki/Silver_sulfide.